Available online at www.sciencedirect.com

ScienceDirect

journal homepage: www.elsevier.com/locate/he

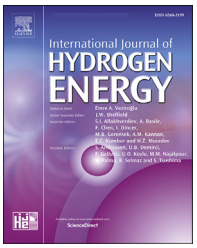

Numerical investigation on pinhole leakage and diffusion characteristics of medium-pressure buried hydrogen pipeline

Yankang Zhang [a], Yilan Yang [a], Fengrong Wu [b], Qianqian Li [a,**], Jinhua Wang [a], Hu Liu [a,*], Defu Che [a], Zuohua Huang [a]

[a] State Key Laboratory of Multiphase Flow in Power Engineering, Xi'an Jiaotong University, Xi'an, People's Republic of China

[b] China Petroleum Pipeline Engineering Corporation, Langfang, People's Republic of China

HIGHLIGHTS

- The trait of buried hydrogen pipe diffusion with a pinhole at the top was studied.
- Factors affecting the diffusion of buried hydrogen pipe leakage were evaluated.
- An equation describing hazard radius on the ground from the pinhole was proposed.

ARTICLE INFO

Article history:
Received 23 October 2022
Received in revised form
26 February 2023
Accepted 17 April 2023
Available online 06 May 2023

Keywords:
Numerical simulation
Hydrogen
Leakage and diffusion
Medium-pressure buried pipeline
Hazard radius

ABSTRACT

Pipeline transportation of hydrogen is by far the most efficient and mature way, but special attention needs to be paid to the diffusion of hydrogen after a pipeline leakage due to the flammable and explosive nature of hydrogen. In this work, numerical simulation of pinhole leakage of the medium-pressure (0.1 up to 0.4 MPa) buried hydrogen pipeline under different conditions was carried out to analyze the effects of pressure, soil properties, pinhole location and pinhole diameter on the diffusion of leakage. The mass flow rate of the leak and the time when the ground surface is first in danger were obtained. Finally, a correlation between hazard radius of ground surface and time was established by multivariate fitting of the quantifiable influencing factors. This correlation aims to provide data support for understanding medium-pressure hydrogen diffusion characteristics and guide evacuation of ground personnel during the actual leakage.

Introduction

As the global economy continuously develops, human demand for energy is increasing [1]. However, the greenhouse effect caused by fossil fuels has had a huge influence on human life. In the last century, the surface temperature of earth has risen by about 1 °C, resulting in a sea level rise of about 20 cm [2]. In order to mitigate its impact on earth, the development and utilization of clean energy sources is urgent.

* *Corresponding author*. State Key Laboratory of Multiphase Flow in Power Engineering, Xi'an Jiaotong University, Xi'an, 710049, People's Republic of China.
** *Corresponding author*.
E-mail addresses: qianqianli@mail.xjtu.edu.cn (Q. Li), epeliuhu@mail.xjtu.edu.cn (H. Liu).
https://doi.org/10.1016/j.ijhydene.2023.04.209

Many clean energy sources, such as solar, tidal and wind energy, are intermittent, requiring energy storage technology to ensure a stable energy supply [3]. Hydrogen not only has the advantages of high thermal value per mass, wide range of sources and zero carbon emissions [4], but also behaves energy storage intermediate, which makes hydrogen the most promising clean energy carrier in the past years [3].

Hydrogen can be stored and transported in different ways, for instance in hydrogen pipelines, high-pressure cylinders, liquid hydrogen storage tanks [5], and through the reaction between hydrogen and liquid organic hydrogen carriers (LOHC) [6]. Among them, hydrogen pipeline transportation is by far the most efficient and mature way for hydrogen transportation in large quantities and over long distances [7]. Moreover, pipeline transportation can also alleviate the problem of uneven regional distribution of renewable energy sources. Especially for China, pipeline transportation of hydrogen will enable the supply of abundant renewable energy from the western region to the eastern region which has greater energy demand [8]. Since the 215 km long distance hydrogen pipeline was first built in Germany in 1938, the total length of hydrogen pipeline in Europe has exceeded 1600 km, and the hydrogen pipeline in the United States has exceeded 2500 km [8]. The construction of hydrogen pipelines is on the rise all over the world.

Although hydrogen has several advantages, its low ignition energy (0.017 MJ), high diffusion coefficient (0.61 cm^2/s), wide combustion range (volume ratio 4%~75%) and explosion range (volume ratio 11%—59%) could cause safety problems that cannot be ignored in practical use [9,10]. Hence, the diffusion behavior of hydrogen in case of pipeline leakage should be investigated as much as possible. Because of the late start of the research on hydrogen pipeline leakage, the classification of hydrogen pipeline leak sizes is still not clear. In this paper, drawing on the classification related to natural gas pipelines, hydrogen pipeline leak sizes are similarly divided into pinhole, hole and rupture, where pinhole implies that the effective diameter of the hole is smaller than or equal to 2 cm and is the most common leak size for pipelines caused by corrosion, external interference, material failure and so on [11]. Moreover, pinhole leaks are difficult to detect and have potential hazards such as the formation of jet fires [12], and therefore both academics and engineers need to pay extra attention to this situation.

To date, scholars have had some achievements in the research of hydrogen leakage and diffusion. Heitsch et al. [13] performed numerical simulations of accidental leakage of hydrogen from a high-pressure pipeline in a hydrogen laboratory to evaluate the formation of hydrogen clouds inside the laboratory. Xie et al. [14] numerically studied the effect of blower ventilation on hydrogen leakage and diffusion to the environment from a hydrogen-fueled vehicle in an emergency situation and determined the critical factors affecting the performance of the blower, blower shape. Shao et al. [15] simulated hydrogen pipeline leakage in utility tunnel to explore the feasibility and safety of placing hydrogen pipelines and concluded that the existing alarm strategy was not yet well developed and needed to be improved. Li et al. [4] conducted simulations of leakage from closed containers with different methane-to-hydrogen concentration ratios. It was found that at low hydrogen ratio (20% and below) the leakage and diffusion of methane-hydrogen mixtures is closer to that of pure methane, and storage and transportation is safer at this methane-to-hydrogen ratio. Zhu et al. [16] established a full-scale experimental system to study the leakage dispersion behavior and concentration distribution of buried hydrogen-doped natural gas pipelines under different leakage conditions with hydrogen-doping ratios (0, 10%, 20%, 30%), leakage pressures (4 MPa, 5.8 MPa) and leakage directions, and identified the characteristics of leakage occurring in the pipeline with different hydrogen-doping ratios. Wilkening et al. [17] simulated the leakage and diffusion of an underground hydrogen pipeline at a pressure of 1.1 MPa to the atmosphere through a 30 cm diameter hole by CFD-ACE considering the ambient wind speed, but the soil was simplified above the hole. Li et al. [18,19] investigated the mean concentration fields of subsonic and underexpanded hydrogen jets by a planar laser Rayleigh scattering (PLRS) diagnostic system, thereby refining the nominal nozzle model and two-layer reduced-order model, to alleviate the trouble of numerical simulations at the shock of underexpanded jet. And when the velocity field of the hydrogen jet obtained from the two-layer model simulation was compared with the experimental data, it was found that the two-layer model can predict the velocity field distribution of the hydrogen jet well, thereby verifying the reliability of the two-layer model [20]. Giannissi et al. [21] tested two nominal nozzle methods for simulating a vertical jet of compressed hydrogen whose temperature is slightly above the saturation liquid temperature and found that the concentration and temperature at the jet centerline are in good agreement with the experimental results. It was also compared with the hydrogen jet at ambient temperature and revealed that the decay rate of the warm jet is faster than that of the cold jet.

Until today, scholars all over the world have not only concerned the hydrogen far-field diffusion and proposed suitable simplified models, but also made elaborate simulations of hydrogen near-field jets. Velikorodny et al. [22] solved the 3-dimensional compressible multicomponent Navier-Stokes equations directly by numerical models to obtain detailed information on the near-field of the high-pressure hydrogen underexpanded jet and gave proper initial conditions for the far-field simulations. Li et al. [23] employed a two-stage modeling approach to model the near- and far-field regions separately for underexpanded hydrogen jet with square and rectangular nozzles of aspect ratios from 1 to 16, with hydrogen stagnation pressure up to 20 MPa. It showed that the effect of nozzle shape on jet spreading should not be neglected, and appropriate scale factors are needed to calculate the decay rate of hydrogen jet concentration. Tolias et al. [24] applied large eddy simulation to a hydrogen subsonic round jet to stagnation environment, and the results demonstrated that even coarse discretization of the hydrogen release area provides acceptable results for hydrogen safety engineering applications.

Most of the research on hydrogen leakage and diffusion focused on hydrogen leakage to the atmosphere, with limited research related to directly buried pipelines. And in a matter of fact, most kinds of pipeline, including gas pipelines, communication cables and power cables, are buried directly

in the soil [15]. Houssin-Agbomson et al. [25] conducted experiments on leakage from a pinhole (12 mm diameter) in a high-pressure hydrogen pipeline in the sandy ground. It was concluded that for a pipeline buried at a depth of 1 m with the pinhole at the top, hydrogen lifts the sand above the pinhole when the hydrogen pressure is 1.7 MPa, while the sand forms a crater over the pinhole for the case of 4.6 MPa. Although the changes in the soil structure above the pipeline during the leakage of buried pipelines at hydrogen pressure of 1.7 MPa and above were analyzed qualitatively, the distribution of the spatial concentration field was not given. In addition, although medium-pressure (0.01≤ pressure≤ 0.4 MPa [26]) hydrogen has now been extensively used for cooling the rotor windings and stator cores of turbine generators in thermal and nuclear power plants, and has a great potential to be used in the future as an alternative to urban gas due to its environmental friendliness, few studies have been conducted on its leakage and diffusion. Therefore, a survey of the leakage dispersion of the medium-pressure buried hydrogen pipeline is essential to explore the changes in the hydrogen concentration field, the hazardous conditions on the ground surface and the loss of hydrogen. In this work, numerical simulations of the leakage and diffusion of a medium-pressure buried hydrogen pipeline in the soil were carried out to give the time for hydrogen to reach the ground and the mass flow rate of hydrogen after leakage under different conditions. A multivariate equation was built for the hazard radius on the ground surface to provide data support for the hydrogen dispersion and guide evacuation of people on the ground during the actual leakage.

Methods

Physical model

To well study the diffusion behavior of hydrogen pipeline leakage buried in the soil, a 3-dimensional model was built. In this model, as shown in Fig. 1, the pipeline with the diameter of 100 mm is 1 m below the ground with the length of 4 m, the width of 4 m and the height of 2 m. In addition, the diameter of the pinhole in the pipeline is defined to be 10 mm.

Mathematical model

To facilitate the calculation, some assumptions need to be made:

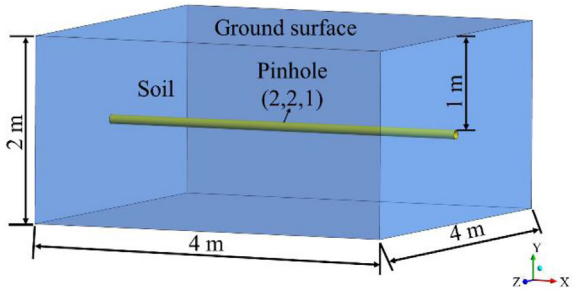

Fig. 1 – Schematic diagram of the physical model.

(1) The soil is an isotropic porous medium which remains unchanged during the leakage process.
(2) The diffusion process is only a mass transfer process.
(3) During leakage, the hydrogen pressure in the pipeline remains unchanged.
(4) Medium-pressure hydrogen can be regarded as ideal gas.
(5) The soil contains only dry air without moisture.

Based on the above assumptions, the governing equations, including continuity conservation equation, momentum conservation equation, the mixed gas density equation and species transport equation, are expressed as follows [27]:

$$\varepsilon\frac{\partial\rho}{\partial t}+\nabla\cdot(\rho v_i)=0 \tag{1}$$

$$\varepsilon\rho\frac{\partial v_i}{\partial t}+\frac{\rho}{\varepsilon^2}(v_i\cdot\nabla)v_i=-\nabla p+\frac{\mu}{\varepsilon}\nabla^2 v_i+\varepsilon\rho g+S_i \tag{2}$$

$$\rho=\frac{p}{RT}\frac{M_v M_a}{[wM_a+(1-w)M_v]} \tag{3}$$

$$\varepsilon\frac{\partial}{\partial t}(\rho w)+\nabla\cdot(\rho w v_g)=\nabla\cdot(\rho D\nabla w) \tag{4}$$

where, ρ is mixed gas density, t is time, v_i is the velocity of gas in the x, y, z directions, ε is soil porosity, w is mass fraction of component, M_a and M_v are respectively relative molecular mass of air and hydrogen, v_g is diffusion velocity of gas in the soil and D is the diffusion coefficient.

In this work, the DES with the Spalart-Allmaras model was adopted as the turbulence model for less computational cost and better convergence to simulate the hydrogen leakage process at pinhole. The Detached Eddy Simulation model (DES) is typically known as the hybrid LES/RANS model. RANS is used for calculations in the boundary layer region, while the LES model is employed for the separated region. The porous media zone was set as a specific fluid zone where the fluid flow was laminar, due to the nature of the soil.

Soil characteristics

Since the soil is assumed to be an isotropic porous medium, the viscous resistance coefficient ($1/\alpha$) and inertial resistance coefficient (C_2), indispensable parameters used to characterize different types of soils, can be simplified as follows [28]:

$$\frac{1}{\alpha}=\frac{150}{D_p^2}\frac{(1-\varepsilon)^2}{\varepsilon^3} \tag{5}$$

$$C_2=\frac{3.5}{D_p}\frac{(1-\varepsilon)}{\varepsilon^3} \tag{6}$$

where, D_p is mean diameter of soil particles. Three main kinds of soil were studied in this paper, and their characteristics are listed in Table 1 [27].

Numerical methods

In this work, commercial software ANSYS FLUENT 2020 R1 was adopted to simulate the leakage and diffusion process of

Table 1 – Characteristics of the soils.

Soil type	Particle diameter D_p (mm)	Porosity ε	Viscous resistance $1/\alpha$ ($1/m^2$)	Inertial resistance C_2 (1/m)
Sandy	0.5	0.25	2.16e+10	3.36e+05
Loam	0.05	0.43	2.45e+11	5.02e+05
Clay	0.01	0.3	2.72e+13	9.07e+06

the pinhole in the directly buried hydrogen pipeline. Because this process is transient, the coupling of the velocity and pressure phrases was solved by PISO algorithm. As assumed in Section Mathematical model, the soil is an isotropic porous medium with abrupt changes in the pressure gradient, so PRESTO! method was used for the discretization of the pressure and the simulation accuracy of the second order upwind discretization format was used for other terms. The time step size was set to be 0.1 s. The number of time steps was 12,000 and the maximum iteration was 110 steps.

Boundary conditions

In case of leakage, the pressure at the pinhole can be considered equal to the pressure in the pipeline [27]. The pressure and temperature in the soil and at the boundary of the soil are atmospheric pressure and 300 K, respectively. The specific boundary conditions are as follows. Pinhole, pipeline sidewall and soil zone were set as pressure inlet, wall and interior respectively, as well as soil boundaries and ground surface were set as pressure outlet. And the interior refers to a surface inside the fluid domain.

Simulation conditions

Present study adopted the control variable method to numerically investigate the diffusion behavior of hydrogen pipeline leakage buried in the soil. The variables are pressure, soil type, pinhole location and pinhole diameter. When the position of the pinhole is at the top, side and bottom of the pipeline, the coordinates of the corresponding pinhole center are (2,1,2), (2,0.95,2.05) and (2,0.9,2), respectively. Specific cases can be seen from Table 2.

Grid independence verification

Structured grid of physical models was generated through ICEM CFD 2020 R1. When meshing, it is necessary to properly refine the meshes in the area near the pipe outer wall and the pinhole, as indicated in Fig. 2(a). To ensure the accuracy and reliability of the numerical simulation, the grid independence was verified using the physical model with the pinhole at the top of the pipeline. According to the grid size, four schemes with grid numbers of 494,344, 730,494, 837,400 and 912,218 were simulated to observe the change of the hydrogen volume concentration fraction at the point (2, 1.5, 2) with time, as shown in Fig. 2(b). When the number of grids is not less than 730,494, the variation of hydrogen volume concentration with time is almost the same. Compared with the scheme with 912,218 grids, the scheme with 730,494 grids has an average difference of 0.4%. Therefore, to ensure the calculation accuracy and reduce the time cost, the scheme of 730,494 grids was selected for subsequent numerical simulation. In this scheme, the minimum volume of the cell is 1.879776×10^{-10} m^3 with a growth rate of 1.2.

Table 2 – Working conditions.

Case	Pressure (MPa)	Soil type	Pinhole direction	Pinhole diameter (mm)
Case 1	0.4	Loam	Top	10
Case 2	0.2	Loam	Top	10
Case 3	0.1	Loam	Top	10
Case 4	0.4	Clay	Top	10
Case 5	0.4	Sandy	Top	10
Case 6	0.4	Loam	Side	10
Case 7	0.4	Loam	Bottom	10
Case 8	0.4	Loam	Top	8
Case 9	0.4	Loam	Top	6

Model validation

So far, few quantitative experiments have been implemented regarding leakage and diffusion of the buried hydrogen pipeline, so the model validation of this study was carried out by comparing with leakage experiments of buried compressed air pipeline and buried diluted natural gas pipeline to demonstrate the reliability of the numerical simulations in terms of leakage mass flow rate as well as concentration fields.

Firstly, the leakage of the buried compressed air pipeline was simulated and compared with the experiments regarding the leakage mass flow rate. According to the experimental scheme [29], a total of 120 sets of experimental conditions, including different burial depths, leakage pressures and pinhole diameters, were performed by Liang. In this paper, a series of experiments, where leakage occurred at different pipeline pressures (10 kPa, 20 kPa, 30 kPa, 40 kPa and 50 kPa) for a compressed air pipeline buried at a depth of 0.8 m and with a pinhole diameter of 4 mm, was chosen to demonstrate the reliability of the model. Based on Liang's experiments, the computational domain is determined to be 4 m × 4 m × 0.8 m, the mean particle diameter of the soil is 0.198 mm as well as a porosity of 0.6. Fig. 3 shows the experimentally measured leakage mass flow rate at different pressures and the corresponding simulated leakage mass flow rate. The maximum difference between the experiments and simulations is 16.4%, and the average difference is 8.5%, suggesting the model is reliable.

Secondly, the buried diluted natural gas pipeline leakage was simulated by comparing the concentration diffusion field with the experiments to further verify the reliability of the simulations. According to the experimental scheme [28,30], the computational domain is a cylinder with a diameter of 10 m and a height of 0.9 m. The burial depth of the leak hole is 0.9 m and the diameter is 5 mm. The gas composition in the pipeline is 2.5 vol% methane and 97.5 vol% air. The mean soil

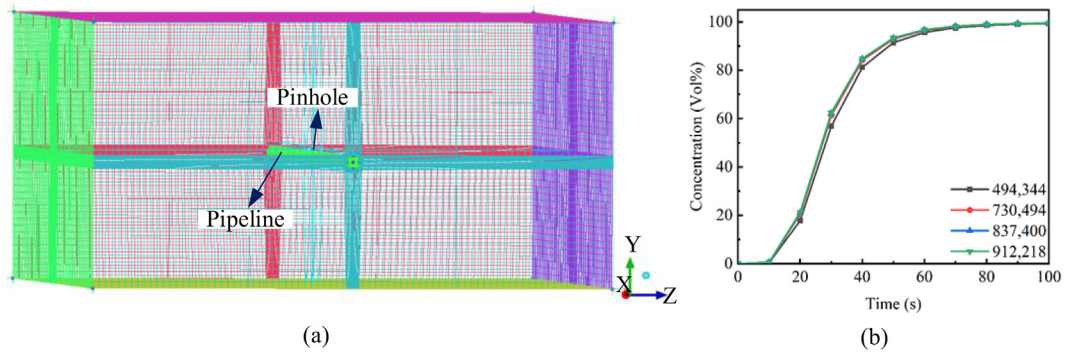

Fig. 2 – Detailed information of grid generation. (a) Structured grid of physical model. (b) Grid independence verification.

porosity is 0.1335, the viscous resistance coefficient is 6.67e+10, and the inertial resistance coefficient is 3.36e+5. Fig. 4 shows the methane volume concentrations of sensor 3 (−1.5, 0, 0.8) and sensor 8 (1, 1, 0.5) over time and the corresponding simulation results for the first 3.5 h of leakage from a natural gas pipeline with leakage volume flow of 12 L/min. The maximum difference between experiment and simulation is 17.9% and the average difference is 8.9%, indicating that the model is reliable.

The main reason for the difference is that the soil is idealized as an isotropic and fixed porous medium in the numerical simulation to simplify the calculation, while in reality the structure of soil may change when leakage occurs, and experimental uncertainty also exists.

Results and discussion

Diffusion process of hydrogen in the soil

Concentration contours

Present study takes Case 1 as the reference condition. Fig. 5 depicts the diffusion of hydrogen in the loam at 10 s, 60 s and 100 s after the leakage of a pinhole in the pipeline. Since the soil is assumed to be an isotropic porous medium, the diffusion of hydrogen above the pinhole can be approximated as a hemisphere. In the first 60 s of the leakage, hydrogen diffuses rapidly in the soil. By 100 s, there is some hydrogen reaching the ground surface. The density of hydrogen is much smaller than that of air, which leads to the hydrogen that leaks out of the pinhole tends to diffuse upward. Therefore, the diffusion of hydrogen above the pinhole plane is stronger than below it.

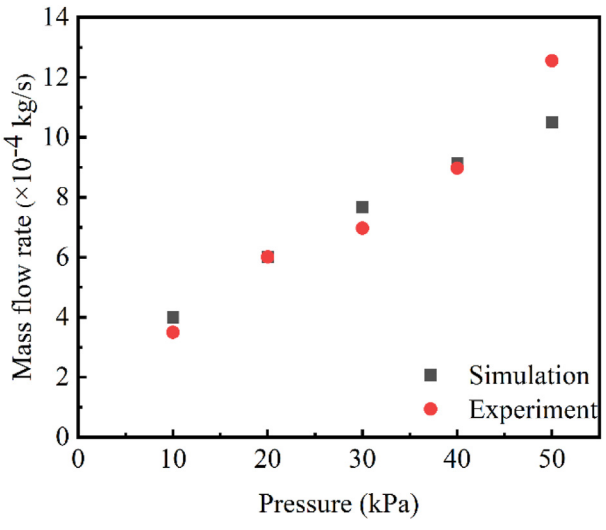

Fig. 3 – Model validation by leakage mass flow of the buried air pipeline.

Hydrogen concentrations at different test points

To better understand the diffusion of hydrogen in the soil, 12 test points at different locations were selected to observe the variation of hydrogen concentration over time at each position, as shown in Fig. 6 which also displays the detailed coordinate information of each point.

Fig. 7(a) indicates the change in hydrogen concentration over 1200 s during the leakage at four test points (test point 1, 2, 7 and 12) along the vertical direction of the pipeline at the center of the pinhole. Compared to test point 2, 7 and 12, test point 1 is the closest to the center of the pinhole, so test point 1 is the first to detect hydrogen and reaches 100% concentration with the shortest time. The hydrogen concentration increases much more slowly as the distance from the test point to the center of the pinhole increases. As illustrated in Fig. 7(b) and (c), at the same height and distance from the test point to the center of the pinhole, the hydrogen concentration changes tend to be the same.

The trend of hydrogen concentration over time at the above 12 test points suggests that when hydrogen is detected, the change of hydrogen concentration at that test point has three stages, namely first a slow increase, then a rapid increase and finally another slow increase. This trend is similar to the concentration change of natural gas in the soil [31].

Hydrogen concentrations at different test lines

Fig. 8(a) presents the perpendicular distance of each test line from the center line of the hydrogen pipeline. As shown in Fig. 8(b), the distribution of hydrogen concentration on the test line is symmetrical along the midpoint of the test line and conforms to a Gaussian distribution. As test line 2 is the closest to the pinhole, the greatest diffusion range of hydrogen can be detected on this line and an area of 100% hydrogen concentration already presents at 100 s of hydrogen leakage.

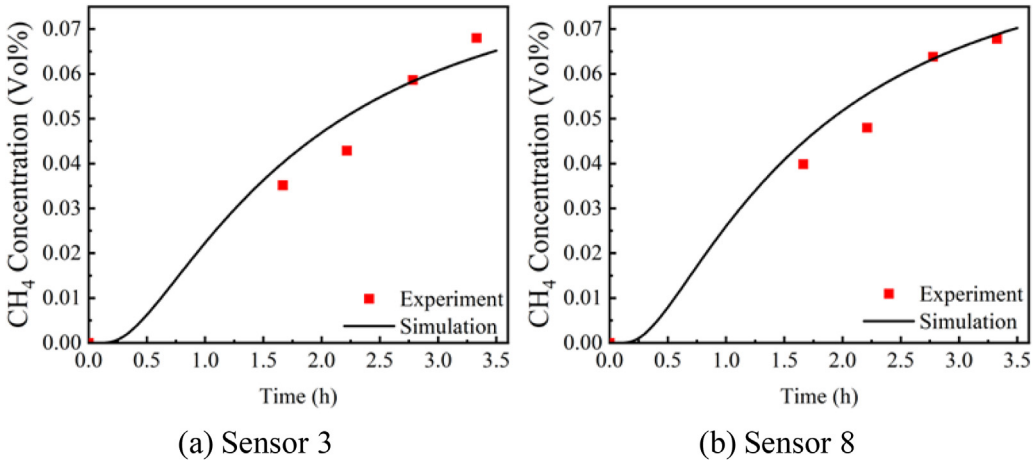

Fig. 4 – Model validation by volume concentration variation of the buried natural gas pipeline.

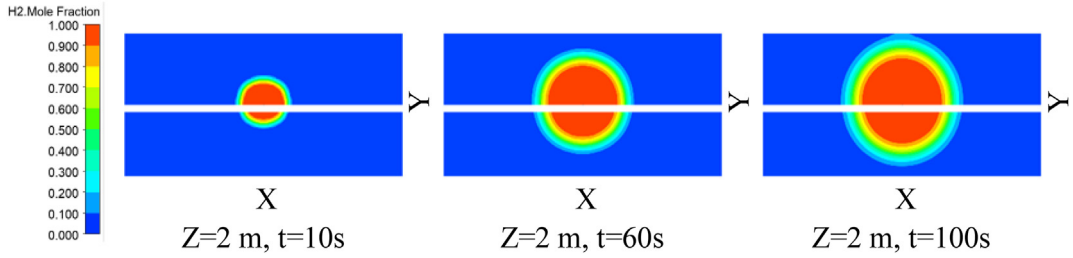

Fig. 5 – The concentration fraction contours of hydrogen over time.

Coordinate: 1(2,1.2,2); 2(2,1.5,2); 3(2,1.5,3); 4(2,1.5,1)
5(1,1.5,2); 6(3,1.5,2); 7(2,0.4,2); 8(2,0.4,3)
9(2,0.4,1); 10(1,0.4,2); 11(3,0.4,2); 12(2,2,2)

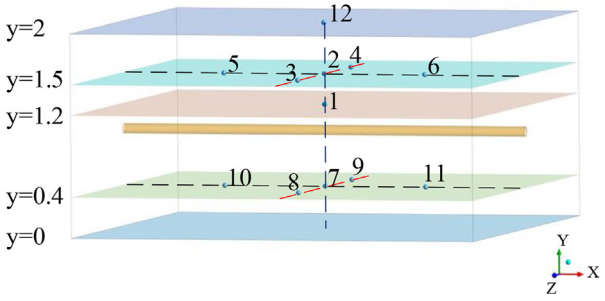

Fig. 6 – Test points in the physical model.

Effects of different factors on hydrogen diffusion in the soil

In this part, the effects of hydrogen pressure, soil type and pinhole location on hydrogen diffusion in the soil are discussed.

Effect of hydrogen pressure

In this section, the effect of different hydrogen pressures on the diffusion of hydrogen in the loam is investigated by comparing Case 1, Case 2 and Case 3.

As shown in Fig. 9, the increase of hydrogen pressure in the pipeline leads to a significant rise in the leakage mass flow rate. When the pipeline pressure is 0.1 MPa, 0.2 MPa and 0.4 MPa, the corresponding leakage mass flow rates at steady state are 1.03×10^{-4} kg/s, 2.56×10^{-4} kg/s and 6.55×10^{-4} kg/s, respectively.

When a pinhole leakage occurs in a buried hydrogen pipeline, ignition or even explosion is more likely to occur above ground than in the soil, due to human activity and the high concentration of oxygen in the air. Therefore, the time when the hydrogen concentration on the ground first reaches the lower flammability limit caused by the pinhole leakage of buried hydrogen pipeline is worthy of attention. Fig. 10 shows the time for the ground surface to first reach the lower flammability limit at different pipeline pressures. It is seen that the time is 272 s when the pipeline pressure is 0.1 MPa, while it is only 85 s at a pipeline pressure of 0.4 MPa. This illustrates that higher pipeline pressure causes shorter time to reach the dangerous state and requires more concern.

Now the international definitions of hazard area and radius are not yet clear [32]. Therefore, in this work, the hazard area is defined as the area where the hydrogen volume concentration on the ground surface is over 4%. And the hazard radius is defined as the average distance between the location of the maximum hydrogen concentration on the ground surface, usually the location where hydrogen first reaches the ground, and the location where the hydrogen volume concentration on the ground surface is 4%. Fig. 11(a) shows the variation of the hazard radius of the ground surface

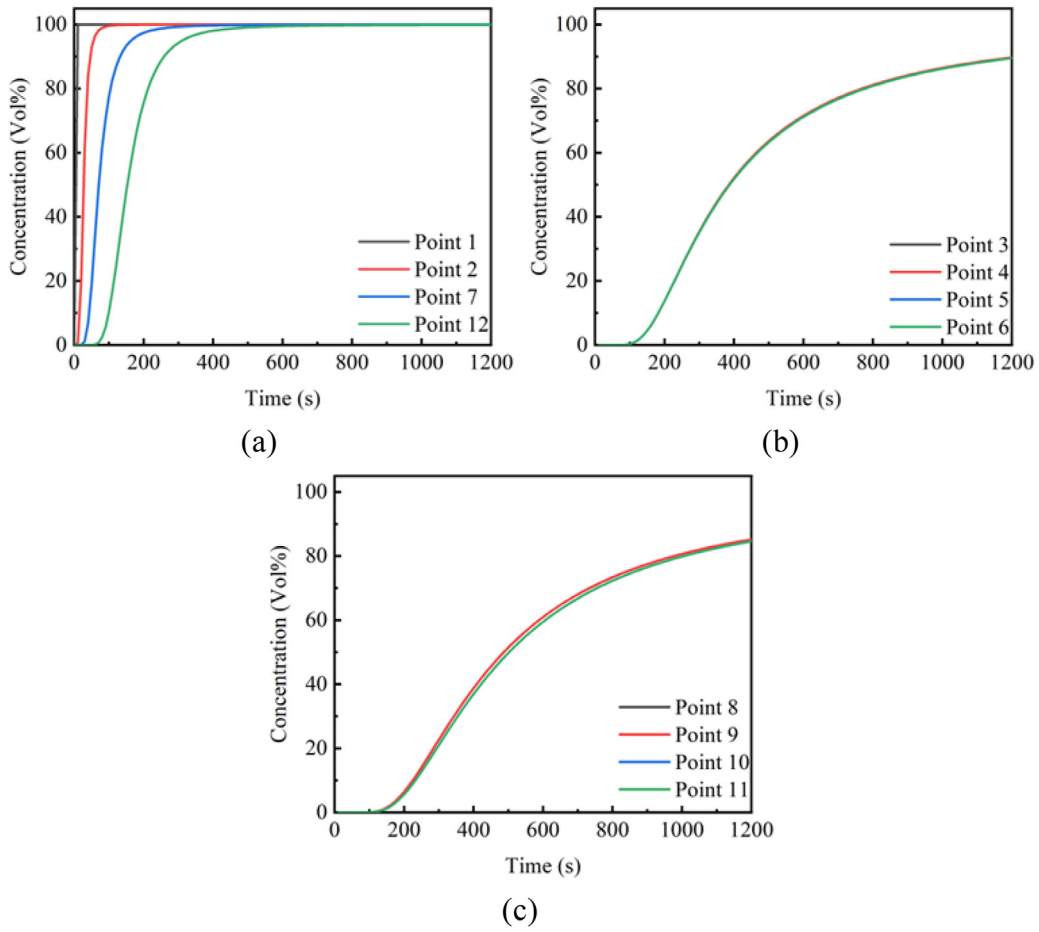

Fig. 7 – The hydrogen concentration over time at different test points.

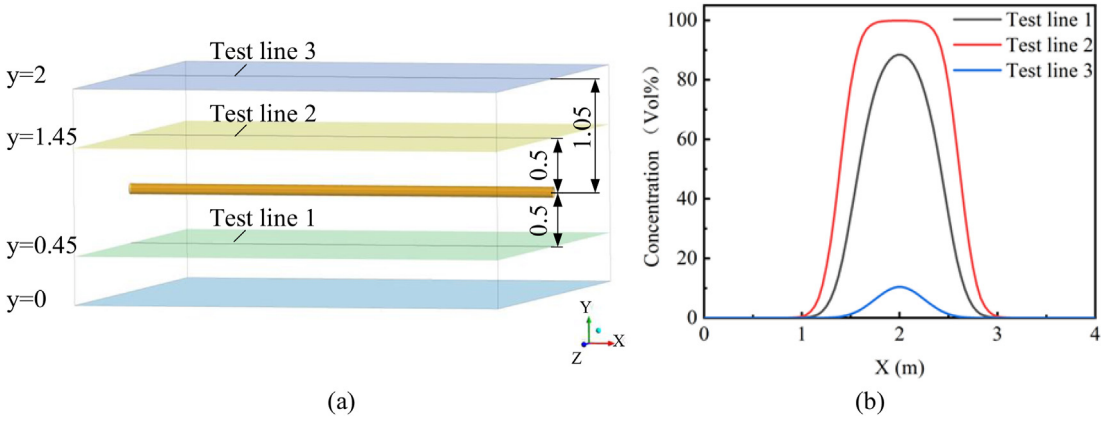

Fig. 8 – Detailed information about test lines. (a) Test lines in the physical model. (b) The hydrogen concentration on different test lines at 100 s of hydrogen leakage.

with time for different pipeline pressures. The hazard radii corresponding to pipeline pressures of 0.4 MPa, 0.2 MPa and 0.1 MPa at 600 s of pinhole leakage are 1.62 m, 1.23 m and 0.87 m, respectively.

Effect of soil type

In this section, the effect of different kinds of soil on the diffusion of hydrogen in the soil is discussed by comparing Case 1, Case 4 and Case 5.

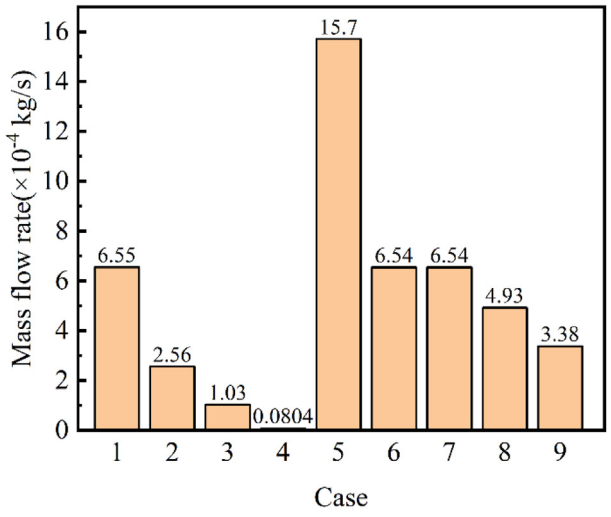

Fig. 9 – Leakage mass flow rates for different conditions.

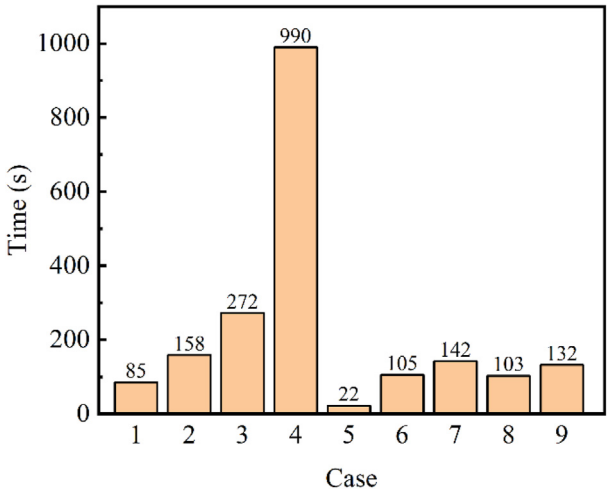

Fig. 10 – The time for the ground to first reach the lower flammability limit under different conditions.

As shown in Fig. 9, when the soil types are loam, clay and sandy, the corresponding leakage mass flow rates are 6.55×10^{-4} kg/s, 8.04×10^{-6} kg/s and 1.57×10^{-3} kg/s, respectively. The wide variation in the properties of different soils leads to a large discrepancy in the hydrogen leakage mass flow rate. Among the three soils, clay has the highest viscous and inertial resistance, and the smallest particle diameter, which greatly retards the hydrogen diffusion speed. On the contrary, the hydrogen diffusion in sandy soil is easy. Specifically, leakage mass flow rate in the sandy soil is 2.40 times that in the loam and nearly 195.27 times that in the clay.

Fig. 10 shows the time for the ground surface to first reach the lower flammability limit for different types of soil. When leakage and diffusion occur in the clay, the time takes 990 s, while it takes only 22 s in the sandy soil.

Fig. 11(b) shows the variation of the hazard radius of the ground surface with time for different soil types. Due to the characteristics of the sandy such as large porosity and less viscosity, hydrogen diffuses the fastest in the sandy soil, and the hazard radius reaches 2 m, the boundary of the calculation domain, after 314 s of leakage. In contrast, within 600 s of leakage in the clay, the hydrogen concentration on the ground is below 4%, which means that the area above the ground is in safe. The distinctive progressive growth trend shown in Case 5 deserves to be studied in depth to determine if it is persistent and if it is due to hydrogen leakage into the sandy ground.

Effect of pinhole location

In this section, the effect of different pinhole locations on the diffusion of hydrogen in the soil is evaluated by comparing Case 1, Case 6 and Case 7.

As shown in Fig. 9, when the location of the pinhole on the hydrogen pipeline is different, regardless of whether it is at the top, bottom or side of the pipeline, the hydrogen leakage mass flow rate is basically constant. In other words, the location of the pinhole in the hydrogen pipeline has nearly no effect on the leakage mass flow rate.

Fig. 10 shows the time for the ground surface to first reach the lower flammability limit at different pinhole location conditions. Although the hydrogen leakage mass flow rate is essentially the same when the pinhole is at different locations, the distance of the pinhole from the ground varies, causing the hydrogen to reach the ground at different times. When the pinhole is at the side of the pipeline, the ground surface is the first to measure the hydrogen volume concentration of 4% at 105 s after the leakage, while it is 142 s when the pinhole is at the bottom. And as mentioned above, it is 85 s when the pinhole is at the top.

Fig. 11(c) shows the variation of the hazard radius of the ground surface with time for different pinhole locations. The hazard radius is the maximum when the pinhole is at the top of the pipeline. At 600 s of leakage, the hazard radii corresponding to the pinholes at the top, side and bottom of the pipeline increase to 1.62 m, 1.56 m and 1.49 m, respectively.

Effect of pinhole diameter

In this section, the effect of different pinhole sizes on the diffusion of hydrogen in the soil is studied by comparing Case 1, Case 8 and Case 9.

As shown in Fig. 9, the leakage mass flow rate increases correspondingly with the increase of the pinhole diameter. The corresponding leakage mass flow rates are 3.38×10^{-4} kg/s, 4.93×10^{-4} kg/s and 6.55×10^{-4} kg/s when the pinhole diameters are 6 mm, 8 mm and 10 mm, respectively.

As shown in Fig. 10, for the same pipeline pressure, as the diameter of the pinhole increases, the time for the ground surface to first reach the lower flammability limit reduces. For the pinhole of 6 mm, 8 mm and 10 mm, the time taken is 132 s, 103 s and 85 s, respectively.

Fig. 11(d) shows the variation of the hazard radius of the ground surface with time for different pinhole diameters. At 600 s of leakage, the hazard radii corresponding to pinhole diameters of 6 mm, 8 mm and 10 mm are 1.35 m, 1.50 m and 1.62 m, respectively. The hazard radius corresponding to different pinhole diameters enters a stable development stage after an initial rapid expansion. The growth rate of each hazard radius in the stable development stage is basically the same.

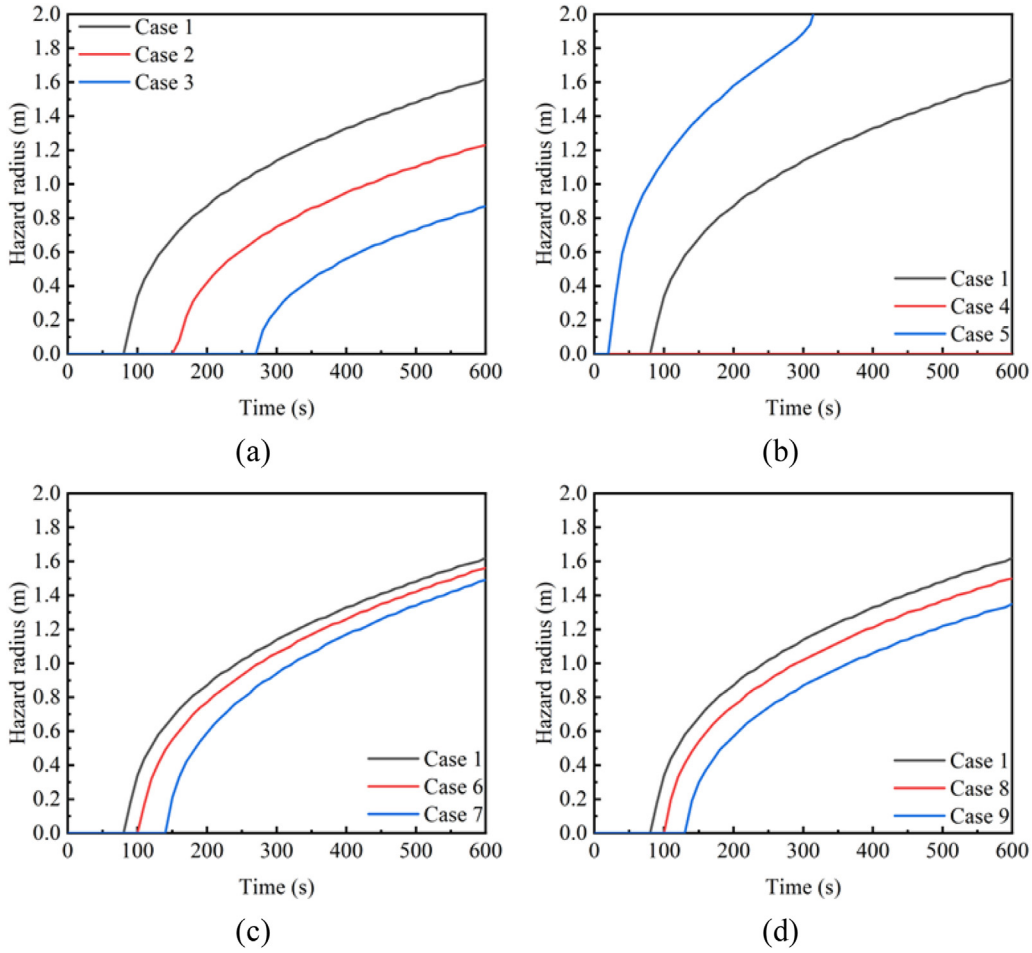

Fig. 11 – The variation of hazard radius over time for different (a) pressures, (b) soil types, (c) pinhole directions, (d) pinhole diameters.

Multivariate fitting of hazard radius

From Section Effects of different factors on hydrogen diffusion in the soil, it is evident that hydrogen pressure, soil type, pinhole location and pinhole diameter all significantly affect the magnitude and development of the hazard radius over time. Therefore, quantifiable parameters including hydrogen pressure, viscous resistance coefficient, inertial resistance coefficients, pinhole diameter and leakage time, are selected in this section for multivariate fitting of the hazard radius to guide the evacuation of ground personnel in the event of the pinhole leakage of buried hydrogen pipeline. As shown in Fig. 11, the hazard radius has a sudden increase in the initial growth phase leading to the existence of a non-differentiable point. Therefore, in order to better fit the hazard radius, the hazard radius fitting is divided into two parts, i.e., the phase when the ground has not yet reached the lower flammability limit and the phase when the hazard radius grows. The first phase indicating that the hydrogen volume concentration on the ground has not yet exceeded 4%. This phase takes different time due to the various leakage conditions, and needs to be qualified. The time when the ground first reaches the lower flammability limit is used as the starting point for the second phase, the growth phase of the hazard radius.

Firstly, the leakage time of the first phase was fitted by quantifiable variables, pipeline pressure, inertial resistance coefficient, viscous resistance coefficient and pinhole diameter, and the fitting equation is as follows:

$$t' = 247.34 - 586.39p + 46.69C_2 - 1.14\frac{1}{\alpha} - 14.52d \tag{7}$$

where, t' is leakage time when the ground first reaches the lower flammability limit (s), p is pipeline pressure (MPa), C_2 is inertial resistance coefficient ($\times 10^5$ 1/m), $\frac{1}{\alpha}$ is viscous resistance coefficient ($\times 10^{10}$ 1/m^2), d is pipeline diameter (mm). The average calculation error in the selected conditions is 6.2% and the coefficient of determination, R^2, is 0.997 with a good model fit.

Secondly, a multivariate nonlinear fit to the hazard radius is proposed with the time after the ground first reaches the lower flammability limit. The fitting equation is as follows:

$$r = 0.42\frac{t^{0.8}}{C_2^{2.5}} - 13.313\frac{p}{\sqrt{\frac{1}{\alpha}}} + 4.954\sqrt{p} + 41.069C_2^{0.1} - 5.903\left(\frac{1}{\alpha}\right)^{0.2} + 0.92d^{0.3} + 0.125\ln(t + 126.297) - 41.36 \tag{8}$$

where, r is hazard radius (m), t is total leakage time (s). The average calculation error in the selected conditions is 10.0%

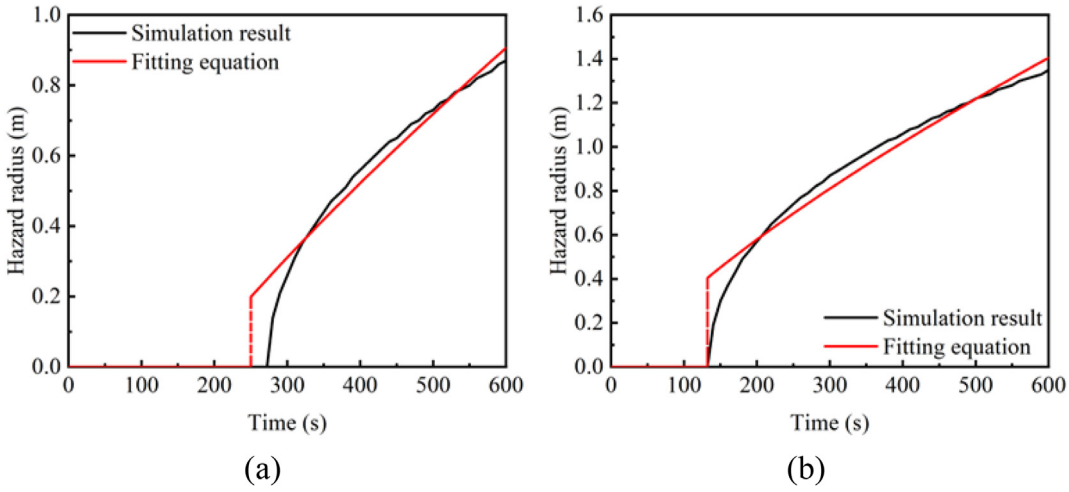

Fig. 12 – Variation of simulated hazard radius and its corresponding fitting radius with time for different working conditions. (a) Case 3. (b) Case 9.

and the coefficient of determination, R^2, is 0.969 with a good model fit.

In this paper, Case 3 and Case 9 are selected as examples for the comparison of the simulation data and the corresponding fitting ones. As shown in Fig. 12, the fitting formula fits the simulation results well except for the initial phase when the hazard radius starts to increase rapidly.

Conclusions

In this work, the diffusion process of pinhole leakage of the medium-pressure buried hydrogen pipeline in the soil was investigated by numerical simulation, and the effects of different variables, pipeline pressure, soil type, pinhole location and pinhole diameter, on diffusion were evaluated. The main observations of this study can be summarized as follows.

(1) Since the soil is assumed to be an isotropic porous medium, the hydrogen diffusion region above the pinhole can be approximated as a hemisphere when the pinhole is at the top of the pipeline.
(2) The leakage mass flow rate of hydrogen gradually grows as the pipeline pressure and pinhole diameter increase. When the hydrogen pipeline is placed in the different types of soil, the leakage mass flow rate is the smallest in the clay and the largest in the sandy soil. The location of the pinhole in the pipeline has little effect on the leakage mass flow rate.
(3) As the pipeline pressure and pinhole diameter increase, the time that is needed to reach the lower flammability limit on the ground becomes shorter. The time to reach the lower flammability limit detected above ground in the clay is 45 times longer that in the sandy soil. Although the change in pinhole location barely affects the hydrogen leakage mass flow rate, the times taken to reach the lower flammability limit above ground are different as the burial depth changes.
(4) The influence of quantifiable parameters, pipeline pressure, viscous resistance coefficient, inertial resistance coefficient and pinhole diameter, on the value and development over time of the hazard radius was quantitatively characterized by developing an equation of hazard radius. This equation will provide useful information for the determination of the hazard area and guide evacuation of personnel in the event of pinhole leakage.

In the near future, the computational domain of the numerical simulations will be further expanded to explore whether there is a boundary for the increase in hazard radius. In addition, a deeper study of hydrogen leakage and diffusion from medium-pressure pipeline in sandy ground is also necessary to figure out whether the trend of the hazard radius is distinctive during long-term leakage. Further, pinhole leakage and diffusion experiments for medium-pressure buried hydrogen pipelines will be implemented to provide the important experimental data to support more accurate numerical simulations. Finally, more variables (burial depth of pipeline, pinhole shape, soil temperature, etc.) will be included in the simulations, thus increasing the simulation samples to obtain a more accurate multivariate fitting equation of hazard radius. It is also meaningful to include the atmospheric environment above the soil surrounding the leaking pipeline in the numerical simulations to guide scholars and engineers visually and convincingly in establishing accident escape mechanisms with respect to pinhole leakage from medium-pressure buried hydrogen pipelines.

Declaration of competing interest

The authors declare that they have no known competing financial interests or personal relationships that could have appeared to influence the work reported in this paper.

Acknowledgements

This work was supported by Science and Technology Plan Program of Yulin (CXY-2021-119), Natural Science Basic Research Program of Shaanxi Province (2020JQ-063) and China Petroleum Pipeline Engineering Corporation.

REFERENCES

[1] Luo Z, Wei C, Wang T, Su B, Cheng F, Liu C, et al. Effects of N2 and CO2 dilution on the explosion behavior of liquefied petroleum gas (LPG)-air mixtures. J Hazard Mater 2021;403:123843.
[2] Dincer I. Technical, environmental and exergetic aspects of hydrogen energy systems. Int J Hydrogen Energy 2002;27:265–85.
[3] Olabi AG, As bahri, Abdelghafar AA, Baroutaji A, Sayed ET, Alami AH, et al. Large-vscale hydrogen production and storage technologies: current status and future directions. Int J Hydrogen Energy 2021;46:23498–528.
[4] Li H, Cao X, Du H, Teng L, Shao Y, Bian J. Numerical simulation of leakage and diffusion distribution of natural gas and hydrogen mixtures in a closed container. Int J Hydrogen Energy 2022;47:35928–39.
[5] Zivar D, Kumar S, Foroozesh J. Underground hydrogen storage: a comprehensive review. Int J Hydrogen Energy 2021;46:23436–62.
[6] Jorschick H, Vogl M, Preuster P, Bösmann A, Wasserscheid P. Hydrogenation of liquid organic hydrogen carrier systems using multicomponent gas mixtures. Int J Hydrogen Energy 2019;44:31172–82.
[7] Zhao B, Li S, Gao D, Xu L, Zhang Y. Research on intelligent prediction of hydrogen pipeline leakage fire based on Finite Ridgelet neural network. Int J Hydrogen Energy 2022;47:23316–23.
[8] Wang H, Tong Z, Zhou G, Zhang C, Zhou H, Wang Y, et al. Research and demonstration on hydrogen compatibility of pipelines: a review of current status and challenges. Int J Hydrogen Energy 2022;47:28585–604.
[9] Li X, Teng L, Li W, Huang X, Li J, Luo Y, et al. Numerical simulation of the effect of multiple obstacles inside the tube on the spontaneous ignition of high-pressure hydrogen release. Int J Hydrogen Energy 2022;47:33135–52.
[10] Salehi F, Abbassi R, Asadnia M, Chan B, Chen L. Overview of safety practices in sustainable hydrogen economy – an Australian perspective. Int J Hydrogen Energy 2022;47:34689–703.
[11] European Gas Pipeline Incident Data Group (EGIG). Report of the European gas pipeline incident data group (period 1970 – 2019). Europe: The Network; 2020.
[12] Liu C, Huang L, Deng T, Jiang H, Wu P, Liu B, et al. Influence of bottom wall on characteristics of jet diffusion flames under cross-wind. Fuel 2021;288:119661.
[13] Heitsch M, Baraldi D, Moretto P. Numerical analysis of accidental hydrogen release in a laboratory. Int J Hydrogen Energy 2010;35:4409–19.
[14] Xie H, Li X, Christopher DM. Emergency blower ventilation to disperse hydrogen leaking from a hydrogen-fueled vehicle. Int J Hydrogen Energy 2015;40:8230–8.
[15] Shao X, Yang S, Yuan Y, Jia H, Zheng L, Liang C. Study on the difference of dispersion behavior between hydrogen and methane in utility tunnel. Int J Hydrogen Energy 2022;47:8130–44.
[16] Zhu J, Pan J, Zhang Y, Li Y, Li H, Feng H, et al. Leakage and diffusion behavior of a buried pipeline of hydrogen-blended natural gas. Int J Hydrogen Energy 2022. https://doi.org/10.1016/j.ijhydene.2022.10.185.
[17] Wilkening H, Baraldi D. CFD modelling of accidental hydrogen release from pipelines. Int J Hydrogen Energy 2007;32:2206–15.
[18] Li X, Hecht ES, Christopher DM. Validation of a reduced-order jet model for subsonic and underexpanded hydrogen jets. Int J Hydrogen Energy 2016;41:1348–58.
[19] Li X, Christopher DM, Hecht ES, Ekoto IW. Comparison of two-layer model for hydrogen and helium jets with notional nozzle model predictions and experimental data for pressures up to 35 MPa. Int J Hydrogen Energy 2017;42:7457–66.
[20] Li X, Chowdhury BR, He Q, Christopher DM, Hecht ES. Validation of two-layer model for underexpanded hydrogen jets. Int J Hydrogen Energy 2021;46:12545–54.
[21] Giannissi SG, Venetsanos AG, Hecht ES. Numerical predictions of cryogenic hydrogen vertical jets. Int J Hydrogen Energy 2021;46:12566–76.
[22] Velikorodny A, Kudriakov S. Numerical study of the near-field of highly underexpanded turbulent gas jets. Int J Hydrogen Energy 2012;37:17390–9.
[23] Li X, Chen Q, Chen M, He Q, Christopher DM, Cheng X, et al. Modeling of underexpanded hydrogen jets through square and rectangular slot nozzles. Int J Hydrogen Energy 2019;44:6353–65.
[24] Tolias IC, Kanaev AA, Koutsourakis N, Glotov VY, Venetsanos AG. Large Eddy Simulation of low Reynolds number turbulent hydrogen jets - modelling considerations and comparison with detailed experiments. Int J Hydrogen Energy 2021;46:12384–98.
[25] Houssin-Agbomson D, Blanchetière G, McCollum D, Saint-Macary C, Mendes RF, Jamois D, et al. Consequences of a 12-mm diameter high pressure gas release on a buried pipeline. Experimental setup and results. J Loss Prevent Proc 2018;54:183–9.
[26] Code for design of city gas engineering GB 50028-2006. China; 2006.
[27] Wang X, Tan Y, Zhang T, Xiao R, Yu K, Zhang J. Numerical study on the diffusion process of pinhole leakage of natural gas from underground pipelines to the soil. J Nat Gas Sci Eng 2021;87:103792.
[28] Bu F, Chen S, Liu Y, Guan B, Wang X, Shi Z, et al. CFD analysis and calculation models establishment of leakage of natural gas pipeline considering real buried environment. Energy Rep 2022;8:3789–808.
[29] Liang J. Research on leakage amount estimation and diffusion characteristics for buried gas pipeline [dissertation]. Qingdao: China University of Petroleum (East China); 2019.
[30] Yan Y, Dong X, Li J. Experimental study of methane diffusion in soil for an underground gas pipe leak. J Nat Gas Sci Eng 2015;27:82–9.
[31] Bu F, Liu Y, Liu Y, Xu Z, Chen S, Jiang M, et al. Leakage diffusion characteristics and harmful boundary analysis of buried natural gas pipeline under multiple working conditions. J Nat Gas Sci Eng 2021;94:104047.
[32] Marangon A, Carcassi M, Engebo A, Nilsen S. Safety distances: definition and values. Int J Hydrogen Energy 2007;32:2192–7.